Oceanic vs Continental Origin of the Paleozoic Habach Formation in the Vicinity of the Felbertal Scheelite Deposit (Hohe Tauern, Austria) A geochemical Approach

By VOLKER HÖCK, HARTWIG KRAIGER & HERBERT LETTNER*)

With 13 Text-Figures and 2 Tables

Salzburg
Eastern Alps
Hohe Tauern
Penninic Zone
Habach Formation
Geochemistry
Paleozoic
Island arc sequence
Ophiolites

Österreichische Karte 1 : 50.000
Blätter 151, 152

Contents

Ozeanische vs kontinentale Entstehung der paläozoischen Habach-Formation in der Nachbarschaft der Scheelitlagerstätte Felbertal (Hohe Tauern, Österreich) Eine geochemische Studie

Zusammenfassung

Die Habachformation des Unterfahrungsstollens der Scheelitlagerstätte Felbertal (Salzburg/Österreich) besteht aus verschiedenen Magmatiten und Sedimenten, die bei der alpinen Metamorphose in Grünschieferfazies bzw. in Amphibolitfazies umgeprägt wurden. Aufgrund des weitgehenden Fehlens urspünglicher Relikte basiert die vorliegende Studie vorwiegend auf geochemischen Untersuchungen. Zwei magmatische Abfolgen konnten unterschieden werden. Die tiefere, Untere Magmatitabfolge – sie besteht im wesentlichen aus feinkörnigen Amphiboliten und untergeordnet intermediären Schiefern und Gneisen sowie aus Hornbenditen – wird als subvulkanischer Teil der ozeanischen Kruste eines "marginal basins" (sheeted dike) interpretiert, mit Intrusionen intermediärer und saurer Zusammensetzung, die aus einem kontinentalen Inselbogenmagmatismus herzuleiten sind.

---

*) Authors' address: Ao. Univ.-Prof. Dr. VOLKER HÖCK, HARTWIG KRAIGER & HERBERT LETTNER, Institut für Geologie und Paläontologie, Universität Salzburg, Hellbrunnerstraße 34, A-5020 Salzburg, Austria.

Die vorwiegend vulkanogene Obere Magmatitabfolge, bestehend aus verschiedenen basischen bis sauren Metavulkaniten mit geringen Metasedimentzwischenlagen, kann als Produkt eines kontinentalen Inselbogens angesehen werden. Im Hangendbereich der Oberen Magmatitabfolge, der sogenannten Habachentwicklung, treten neben dominierenden Metasedimenten einzelne Amphibolite mit Intraplattencharakteristik auf.

Folgendes Entwicklungsmodell wird vorgeschlagen: Im Bereich eines älteren Inselbogens kommt es zur Bildung eines „marginal basins" als dessen Teil die Untere Magmatitabfolge angesehen wird. Eine spätere Schließung des Beckens führt zu einer teilweisen Obduktion der ozeanischen Kruste und zu einem Zergleiten des Krustenpakets. Auf den „sheeted dike" Komplex der Unteren Magmatitabfolge werden in der Folge kalkalkalische (z.T. shoshonitische) Vulkanite des kontinentalen Inselbogens der Oberen Magmatitabfolge abgelagert. Gleichzeitig intrudieren kalkalkalische Schmelzen die Untere Magmatitabfolge. Das Ende der Subduktion führt einerseits zum Ausklingen des Vulkanismus, andererseits zur verstärkten Ablagerung von tonigen Sedimenten (Habachphyllitentwicklung) und zum Auftreten eines basischen Intraplattenvulkanismus.

Abstract

The Habach Formation exposed in the "Unterfahrungsstollen" of the Felbertal scheelite deposit (Salzburg/Austria) consists of several types of former magmatic and sedimentary rocks metamorphosed into greenschist to amphibolite facies during the Alpine orogeny. Due to the lack of primary features the following interpretation is based mainly on a geochemical investigation. Two different magmatic sequences can be distinguished. The Lower Magmatic Sequence (LMS) is essentially made up of fine-grained amphibolites. In addition, different types of intermediate to acidic schists and gneisses and, restricted to the basal sections, hornblendites occur. The LMS is interpreted as sheeted dike-complex originating from an oceanic marginal basin. However, the intermediate to acidic intercalations are considered to be intrusive and related to a continental island arc magmatism. The Upper Magmatic Sequence (UMS) with predominant metavolcaniclastic rocks intercalated by minor metasediments has been formed in a continental island arc setting. On top of the UMS metasediments ("Habachphyllitentwicklung") prevail over metavolcanic rocks. Rare amphibolites indicate a final within-plate magmatism.

The following geological model is proposed: A marginal basin is established in the area of an older island arc. The LMS is considered to be a remnant of this basin. Subsequent closure of the basin led to obduction and splitting up of the oceanic crust. Calc-alkaline to shoshonitic volcaniclastics (UMS) were deposited on the sheeted dike-complex (LMS). Contemporary calc-alkaline dikes feeding the UMS were found intruding the LMS. The decrease in island arc volcanism was associated with an increase in argillaceous sedimentation and with a basic within-plate magmatism.

1. Introduction

The Paleozoic Habach Formation is part of the Tauern Window, the largest and most important Penninic window in the Eastern Alps. The central part of the Window is divided into two lithological units (FRASL, 1958): the "Zentralgneise" and the "Schieferhülle" including the Altkristallin Formation, the Habach Formation and the Permo-Mesozoic formations (Fig. 1). The former is built up by metamorphosed Variscan granitoids, the latter of Precam-
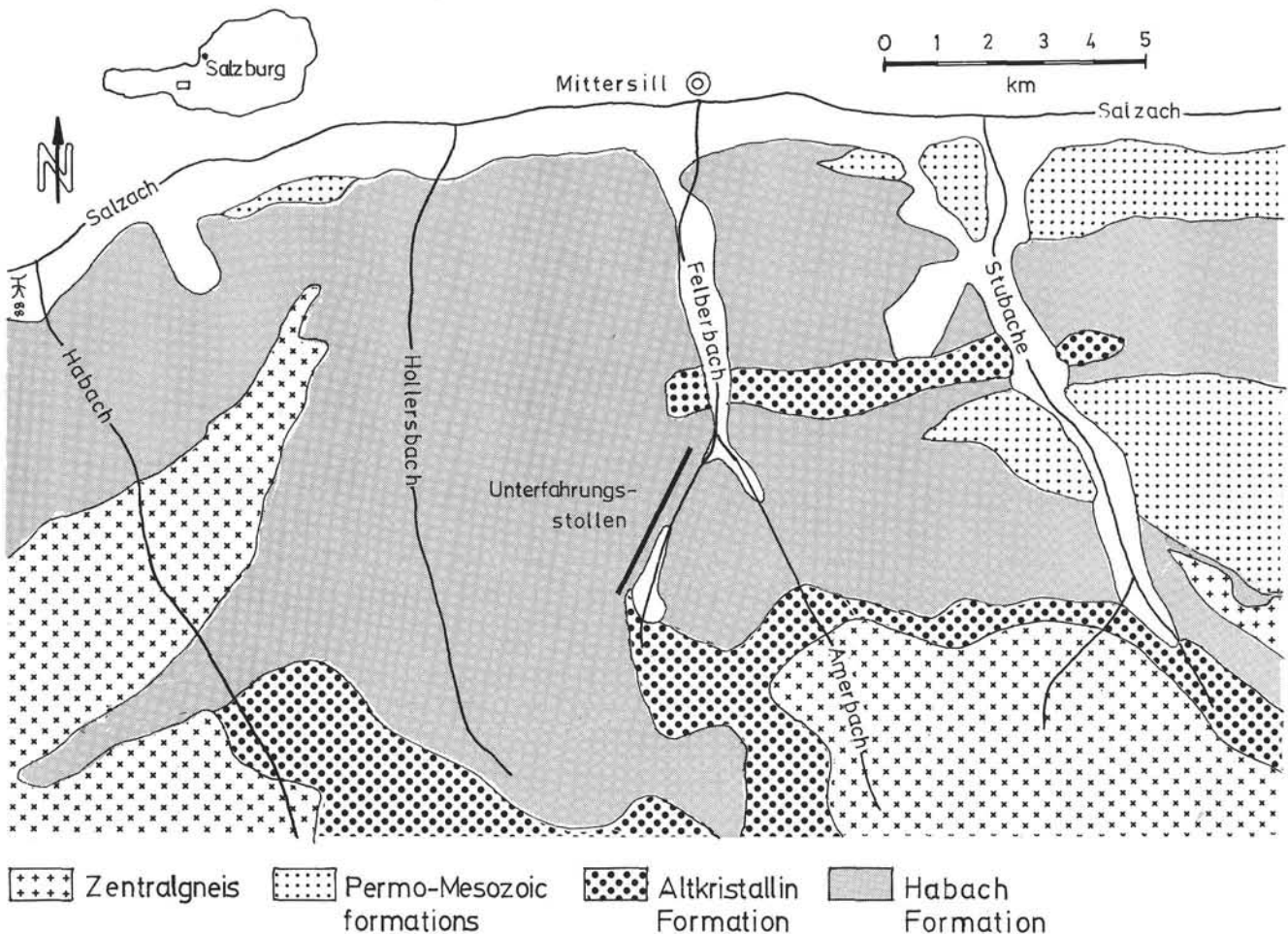

Fig. 1.
Geological sketch-map of the northern part of the "Mittlere Hohe Tauern" including the position of the "Unterfahrungsstollen" of the Felbertal scheelite deposit. The Altkristallin Formation , the Habach Formation and the Permo-Mesozoic formations build up the "Schieferhülle".

brian (?, compare REITZ & HÖLL, 1988), Paleozoic and Mesozoic metamagmatites and metasedimentary rocks. The "Altkristallin" Formation, which consists of garnet-bearing banded amphibolites, schists and migmatic gneisses and the Habach Formation, which contains basic to acidic metamagmatites and pelitic to psammitic metasediments are considered as forming the pre-Permian parts of the Schieferhülle.

During the last few years the Habach Formation has been investigated petrographically and geochemically in some detail by numerous authors. HÖLL, (1975) divided the Habach Formation of the Felbertal scheelite deposit into three units: the "Basisschieferfolge", the "Eruptivgesteinsfolge" and the "Habachphyllitentwicklung". STEYRER (1982, 1983) studied the Habach Formation on its type locality in the Habach valley and interpreted the sequence as a product of an orogenic calc-alkaline volcanism. PESTAL, (1983), HÖCK & PESTAL (1990) considered it as an island arc sequence deposited on perhaps thin continental crust. STEYRER & HÖCK (1985) proposed a back-arc basin situated close to an Early Paleozoic continent. On the contrary, FRISCH & RAAB (1987) interpreted the metamagmatites partly as back-arc basin basalts, partly as primitive island arc volcanic rocks. In the area of the Knappenwand SEEMANN & KOLLER (1989) argued for an island arc environment.

The aim of this study is to contribute to the clarification of the sometimes conflicting results. A newly driven adit within the Felbertal scheelite mine (the so-called "Unterfahrungsstollen"; Fig. 1) presents a favourable opportunity to investigate a continuous profile through the Habach Formation. Therefore it was hoped to gain additional insights into the internal structure on the Habach formation and to improve the interpretation of the geological and geochemical data in terms of geotectonic environments. The present study is based on a detailed geological, petrographic and geochemical investigation in the area of the Felbertal scheelite mine (KRAIGER, 1987) and presents the main geochemical results. Geological and petrographic data have been presented elsewhere (KRAIGER, 1989) and will be only shortly reviewed here.

Recently HÖCK (1993) presented an overview of the Habach Formation, separating it into three subunits including

a) ophiolitic rocks,
b) an island arc volcanic sequence and
c) the Eiser Sequence ("Biotitporphyroblastenschiefer").

The conclusions reached by HÖCK (1993) are in good agreement with the present study.

2. Geological Setting

The "Unterfahrungsstollen" within the pre-Permian formations, shown in Fig. 1, cuts all three lithological units described by HÖLL (1975) on a length of 3500 meters. Based on detailed underground mapping and petrographic studies KRAIGER (1987, 1989) distinguished three lithological units, from bottom to top:

O "Basisschieferfolge" (BSF)
O Lower Magmatic Sequence (LMS)
O Upper Magmatic Sequence and "Habachphyllitentwicklung" (UMS + HPhE).

Compared to HÖLL's classification (1975), the "Eruptivgesteinsfolge" is split up into two units, the LMS and the UMS, being combined with the HPhE.

The rocks of all three units usually strike NE–SW and dip NW. The Alpine metamorphism reached the temperature range of the low-grade amphibolite facies. A pre-Alpine thermal event has not been observed so far (KRAIGER, 1987).

A columnar section of these three subunits in the "Unterfahrungsstollen" is given in Fig. 2. For a detailed petrographic description the reader is referred to KRAIGER (1989).

2.1. "Basisschieferfolge"

The BSF of the "Unterfahrungsstollen", lying at the base of the investigated sequence (Fig. 2) is composed of metasediments (micaschists, paragneisses and quartzites) and some amphibolites and leucocratic gneisses (KRAIGER, 1989; GILG et al. 1989). The BSF is generally identical with the "Biotitporphyroblastenschiefer" of PESTAL (1983) and the Eiser sequence of HÖCK (1993). It has not been investigated in detail.

2.2. Lower Magmatic Sequence

The LMS rests tectonically on the BSF (PESTAL, 1983; KRAIGER 1987). The approximately 800 m thick sequence is mainly built up by different types of metamagmatites (Fig. 2), the most abundant being fine-grained amphibolites. Medium-grained amphibolites and amphibolites with hornblende phenocrysts are of minor extent. Layered or lense-shaped basic-intermediate (plagioclase amphibolite, (garnet)-hornblende-biotite-plagioclase schists), intermediate (biotite gneiss) and acidic (albite gneiss) rocks occur subordinately. In addition small layers of ultramafic hornblendites can be found.

Based on the uniform lithology of the fine-grained amphibolites, the absence of volcaniclastic and sedimentary rocks the non-plutonic section of the LMS is thougt to be of subvolcanic origin. This is supported by the occurrence of medium-grained amphibolites interpreted as gabbro-veins or screens and of hornblenditic rocks (former clinopyroxenites). As KRAIGER (1987, 1989) pointed out, most of the basic to intermediate and intermediate to acidic rocks are considered to be intrusive in character, forming dikes in the fine-grained amphibolites.

2.3. Upper Magmatic Sequence and "Habachphyllitentwicklung" (UMS and HPhE)

The UMS rests unconformably on the LMS. The sequence is mainly made up of basic to acidic metavolcanic rocks and contains metasedimentary rocks only to a minor extent (Fig. 2). In its uppermost section (HPhE), the metasedimentary rocks (dark phyllites, quartzites) prevail over metavolcanic rocks. The whole sequence is at least 650 m thick.

Among the metavolcanic rocks basic and basic-intermediate rocks such as biotite-rich amphibolite, chlorite-albite schists, prasinites, are less frequent than intermediate to acidic rocks (biotite-epidote-albite schists, muscovite-epidote-albite schists, muscovite-albite gneiss). All of these rocks are generally banded at a mm- to dm-scale.
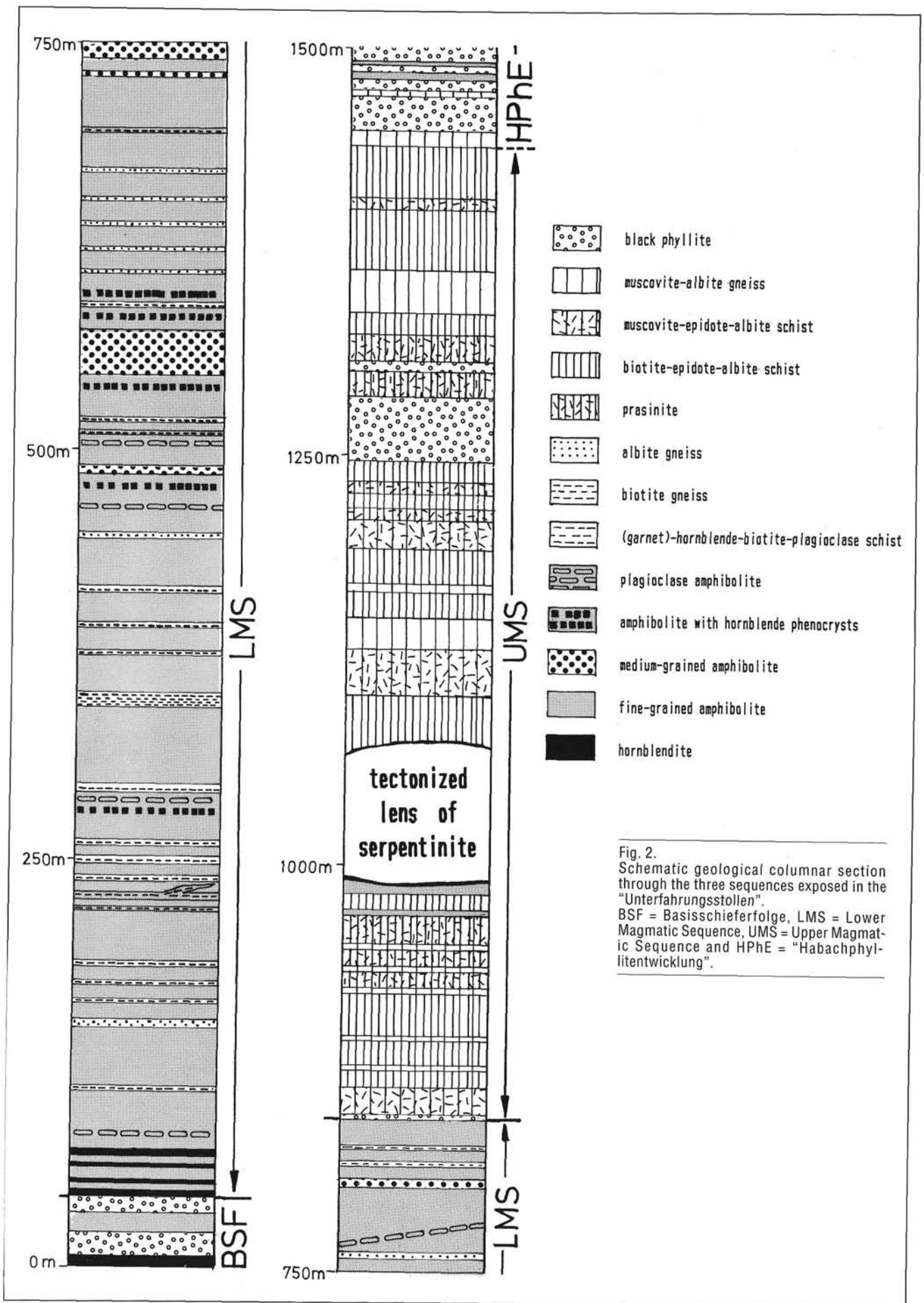
Fig. 2.
Schematic geological columnar section through the three sequences exposed in the "Unterfahrungsstollen".
BSF = Basisschieferfolge, LMS = Lower Magmatic Sequence, UMS = Upper Magmatic Sequence and HPhE = "Habachphyllitentwicklung".

Legend:

- black phyllite
- muscovite-albite gneiss
- muscovite-epidote-albite schist
- biotite-epidote-albite schist
- prasinite
- albite gneiss
- biotite gneiss
- (garnet)-hornblende-biotite-plagioclase schist
- plagioclase amphibolite
- amphibolite with hornblende phenocrysts
- medium-grained amphibolite
- fine-grained amphibolite
- hornblendite

Pseudomorphs after primary plagioclase, clinopyroxene, apatite and volcanic glass have been described by KRAIGER (1987, 1989).

3. Geochemistry

Geochemical data have been obtained from 65 whole rock samples from the two magmatic cycles (LMS and UMS + HPhE). Representative analytical results are given in Tab. 1 and 2. Analyses of major elements were carried out by means of an electron microprobe (type Cambridge MK5), trace elements by Philips PW 1400 XRF and REE by neutron-activation analysis. The glass pellets (for EMP) were measured at 20 kV and 50 nA, trace elements were determined on powder pellets at 60 kV and 45 mA. Major elements finally were corrected according to the method described by BENCE & ALBEE (1968) and trace elements

analyses according to NISBET et al. (1979). The REE including Ta and Hf were determined by INAA and gamma spectroscopy.

Geochemical alteration of the rocks from the Hohe Tauern during the Alpine metamorphism has been proven to be insignificant with the exception of fluid phases (FRASL, 1960; HÖLL, 1975; BICKLE & PEARCE, 1975; HÖCK & MILLER, 1987). However, some alterations by postmagmatic processes in the Paleozoic magmatic rocks, especially in gabbros, must be taken into account. Influence of the W-mineralisation on the geochemical data can be observed only at the base of the LMS. Particularly the Rb concentration (see below) exhibits locally a significant enrichment, which seems to be typical of the mineralized zones (KRAIGER, 1987).

Owing to the striking petrographic differences between the rocks of LMS and UMS, the two sequences are discussed separately.

Table 1.
Selected geochemical analyses from the LMS.
1 = hornblendite; 2,3 = medium-grained amphibolite (metagabbro?); 4,5,6 = fine-grained amphibolite; 7 = amphibolite with hornblende phenocrysts; 8,9 = plagioclase amphibolite; 10,11 = (garnet)-hornblende-biotite-plagioclase schist; 12,13,14 = biotite gneiss; 15 = albite gneiss.

Sample	1 U215	2 U213D	3 U367	4 U230	5 U268	6 U411	7 U291	8 U261	9 U424	10 U252	11 U412	12 U304	13 U334	14 U207	15 U253
SiO2	48.98	53.79	51.53	52.17	51.32	50.18	51.31	56.94	57.22	53.75	53.98	61.57	61.17	70.85	75.73
TiO2	0.12	0.57	2.35	1.41	1.07	1.13	0.66	0.78	0.79	1.21	0.77	0.59	0.99	0.31	0.11
Al2O3	3.52	14.63	16.88	14.47	16.11	15.68	15.25	16.59	16.31	13.75	17.28	16.73	16.90	14.95	11.72
FeO	6.95	7.43	10.58	9.75	8.81	8.65	7.92	6.51	6.82	6.91	6.56	5.15	5.76	2.71	3.38
MnO	0.23	0.13	0.22	0.21	0.17	0.14	0.22	0.14	0.12	0.10	0.10	0.11	0.13	0.03	0.00
MgO	18.32	7.97	4.53	7.00	7.61	8.33	8.35	4.03	4.76	6.63	5.01	2.93	1.86	1.35	0.50
CaO	14.62	8.02	7.41	10.53	9.90	11.29	9.92	7.53	7.93	6.46	7.11	4.91	5.47	3.10	1.57
Na2O	0.37	3.02	2.95	1.91	2.38	2.40	3.34	3.35	3.07	1.99	3.61	3.42	4.79	2.36	5.16
K2O	0.09	0.19	1.56	0.73	0.95	0.14	0.86	1.55	0.94	4.03	1.47	2.46	1.32	2.10	0.18
P2O5	0.03	0.05	0.18	0.10	0.04	0.09	0.26	0.32	0.41	0.57	0.42	0.26	0.32	0.07	0.00
H2O	5.77	3.50	1.05	1.21	1.30	1.45	1.73	2.05	1.17	4.01	3.26	1.10	0.88	1.87	0.96
Total	99.00	99.30	99.24	99.49	99.66	99.48	99.82	99.79	99.54	99.41	99.57	99.23	99.59	99.70	99.31
Nb	0	2	4	3	2	2	10	12	13	20	13	16	18	11	5
Zr	5	52	78	91	56	73	102	183	195	379	208	218	273	154	169
Y	7	15	30	35	33	26	17	21	22	25	21	18	29	13	36
Sr	26	141	182	202	172	148	337	706	574	258	510	638	490	302	60
Rb	0	9	181	110	148	28	191	255	94	493	136	378	167	128	5
Ba	10	32	491	127	183	69	237	1010	812	1369	460	1644	781	992	14
Ni	125	33	15	59	104	86	88	27	27	169	26	29	13	4	10
Cr	2494	648	83	237	416	395	268	45	174	359	72	53	122	108	35
Co	n.d.	n.d.	32	n.d.	53	44	38	n.d.	46	n.d.	16	13	12	n.d.	7
Sc	n.d.	n.d.	44	n.d.	52	46	45	n.d.	30	n.d.	17	13	13	n.d.	10
Ta	n.d.	n.d.	0.26	n.d.	0.20	0.10	0.40	n.d.	0.84	n.d.	0.37	0.54	0.94	n.d.	0.26
Hf	n.d.	n.d.	2.60	n.d.	1.63	2.04	2.84	n.d.	5.41	n.d.	3.64	5.54	6.50	n.d.	4.36
La	n.d.	n.d.	6.36	n.d.	2.00	2.93	21.56	n.d.	61.81	n.d.	9.40	62.66	52.59	n.d.	20.73
Ce	n.d.	n.d.	18.45	n.d.	11.12	11.36	44.69	n.d.	111.03	n.d.	109.34	119.75	121.63	n.d.	54.20
Nd	n.d.	n.d.	13.97	n.d.	4.42	n.d.	21.01	n.d.	52.83	n.d.	43.83	43.13	52.91	n.d.	24.07
Sm	n.d.	n.d.	3.20	n.d.	2.50	4.68	n.d.	n.d.	10.77	n.d.	11.58	9.81	5.33	n.d.	6.20
Eu	n.d.	n.d.	1.40	n.d.	1.08	1.00	1.58	n.d.	2.20	n.d.	1.57	1.49	2.19	n.d.	0.78
Tb	n.d.	n.d.	0.91	n.d.	0.60	0.34	1.20	n.d.	1.12	n.d.	0.27	0.27	1.02	n.d.	0.35
Yb	n.d.	n.d.	3.34	n.d.	2.76	2.74	1.53	n.d.	2.10	n.d.	1.36	2.08	2.82	n.d.	3.26
Lu	n.d.	n.d.	0.46	n.d.	0.42	0.57	0.25	n.d.	0.28	n.d.	0.23	0.32	0.32	n.d.	0.61

Table 2.
Selected geochemical analyses from the UMS.
1,2 = biotite amphibolite; 3 = prasinite; 4 = chlorite-albite schist; 5,6 = biotite-epidote-albite schist; 7 = muscovite-epidote-albite schist, 8 = muscovite-albite gneiss.

	1	2	3	4	5	6	7	8
Sample	U26	U155	U173	U96	U39	U181	U191	U72
SiO2	51.14	40.27	50.47	48.31	50.68	52.87	51.39	69.94
TiO2	2.08	1.80	0.84	1.81	0.65	0.88	0.70	0.34
Al2O3	15.88	7.95	17.49	12.99	15.82	17.42	20.66	14.73
FeO	10.87	10.09	8.01	8.25	5.59	7.37	5.84	2.18
MnO	0.20	0.21	0.13	0.13	0.13	0.11	0.09	0.04
MgO	5.26	11.43	5.92	8.02	2.86	3.66	2.22	1.51
CaO	8.02	14.23	7.89	6.67	10.98	7.69	9.72	2.08
Na2O	4.23	0.51	4.12	2.53	4.69	3.29	2.31	4.68
K2O	0.47	2.05	1.27	2.40	1.66	2.34	2.76	2.10
P2O5	0.32	2.52	0.63	0.26	0.40	0.47	0.59	0.12
LOI	1.67	7.59	3.36	8.25	5.70	3.13	3.25	2.39
Total	100.14	98.65	100.13	99.62	99.16	99.23	99.53	100.11
Nb	6	60	8	34	8	16	9	13
Zr	120	702	136	133	177	120	159	163
Y	35	45	21	23	11	22	16	14
Sr	284	1265	1163	183	817	1029	2195	203
Rb	6	109	50	98	41	109	105	40
Ba	86	1549	896	630	883	1436	1367	1424
Ni	24	202	26	188	27	15	22	-2
Cr	71	692	77	329	91	98	41	49
Co	n.d.	n.d.	42	n.d.	n.d.	n.d.	19	n.d.
Sc	n.d.	n.d.	32	n.d.	n.d.	n.d.	14	n.d.
Ta	n.d.	n.d.	0.50	n.d.	n.d.	n.d.	0.52	n.d.
Hf	n.d.	n.d.	4.77	n.d.	n.d.	n.d.	5.29	n.d.
La	n.d.	n.d.	52.47	n.d.	n.d.	n.d.	73.89	n.d.
Ce	n.d.	n.d.	107.40	n.d.	n.d.	n.d.	147.77	n.d.
Nd	n.d.	n.d.	60.50	n.d.	n.d.	n.d.	59.97	n.d.
Sm	n.d.	n.d.	9.80	n.d.	n.d.	n.d.	12.64	n.d.
Eu	n.d.	n.d.	2.92	n.d.	n.d.	n.d.	2.61	n.d.
Tb	n.d.	n.d.	0.73	n.d.	n.d.	n.d.	0.38	n.d.
Yb	n.d.	n.d.	2.06	n.d.	n.d.	n.d.	1.89	n.d.
Lu	n.d.	n.d.	0.24	n.d.	n.d.	n.d.	0.26	n.d.

It should be noted that the major element values given in the text and in the diagrams have been recalculated on an anhydrous basis.

3.1. Lower Magmatic Sequence

3.1.1. Basic members

Among the metabasites of the LMS four rocktypes can be distinguished: hornblendite, medium-grained amphibolite, fine-grained amphibolite and amphibolite with hornblende phenocrysts.

Coarse-grained hornblenditic rocks form small layers near the base of the profile (Fig. 2) and are restricted to the vicinity of the BSF. In many parts of the mine, but not in this particular profile, they are in close connection with the coarse-grained amphibolites, interpreted as metamorphosed pegmatitic gabbros (KRAIGER, 1987). Geochemically, the hornblenditic rocks (Tab. 1;1) are characterized by low SiO_2, contents between 50–52 %, TiO_2 (0.15 %),

Al_2O_3 (3.5–7 %), Zr (5–8 ppm), Y (7 ppm) but high MgO (15–18 %), CaO (11–15 %), Cr (1200–2500 ppm). They chemically resemble clinopyroxenites as described by BECCALUVA et al. (1984) and HAWKINS (1980). The geological situation combined with petrographical and geochemical evidence indicates a cumulate origin (clinopyroxenite) for the hornblendites.

The coarse-grained amphibolites ("Grobkornamphibolite"), former isotropic gabbros, which are widespread in the mine and its vicinity, are missing in the particular profile investigated.

Medium-grained amphibolites occurring frequently in the LMS (Fig. 2.) are also believed to be at least partly derived from former plutonic rocks. From the structural and petrographical point of view (KRAIGER, 1989) they are interpreted as gabbro-screens. They can be divided into two groups: one with low Ti, Zr, Y and high Cr, Ni contents (Tab. 1;2), the other characterized by high TiO_2 (2–2.5 %) but low in Cr content (50–82 ppm, Tab. 1;3) indicates some Fe- and Ti-enrichment trends.
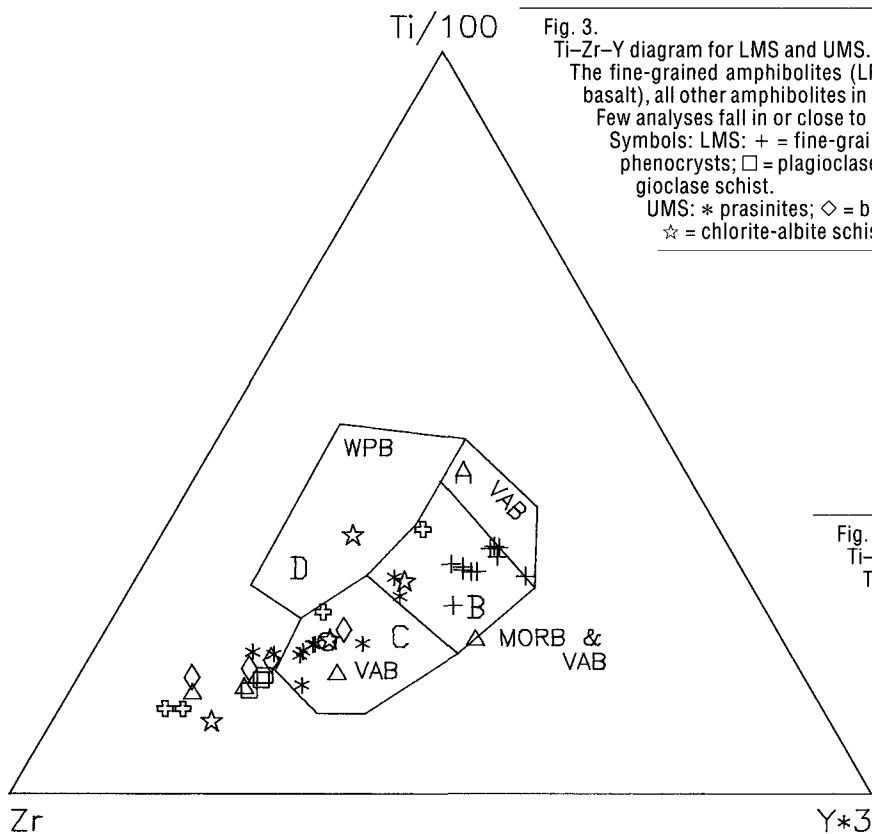
Fig. 3.
Ti–Zr–Y diagram for LMS and UMS.
The fine-grained amphibolites (LMS) plot in field B (MORB and VAB = volcanic arc basalt), all other amphibolites in B and C (VAB) or outside field C towards the Zr apex. Few analyses fall in or close to field D (within-plate basalt = WPB).
Symbols: LMS: + = fine-grained amphibolite; ○ = amphibolite with hornblende phenocrysts; □ = plagioclase amphibolite; △ = (garnet)-hornblende-biotite-plagioclase schist.
UMS: ∗ prasinites; ◇ = biotite-epidote-albite schist; ✢ = biotite amphibolite; ☆ = chlorite-albite schist.

Fig. 4.
Ti–Zr diagram for LMS and UMS.
The fine-grained amphibolites (LMS) plot in the MORB field, most other volcanic rocks in the field of arc lavas and a few chlorite-albite schists and biotite amphibolites in the within-plate lava field.
Symbols: LMS: + = fine-grained amphibolite; × = plagioclase amphibolite; ○ = (garnet)-hornblende-biotite-plagioclase schist; □ = biotite gneiss (group II).
UMS: as in Fig. 3; ✿ = muscovite-albite gneiss.
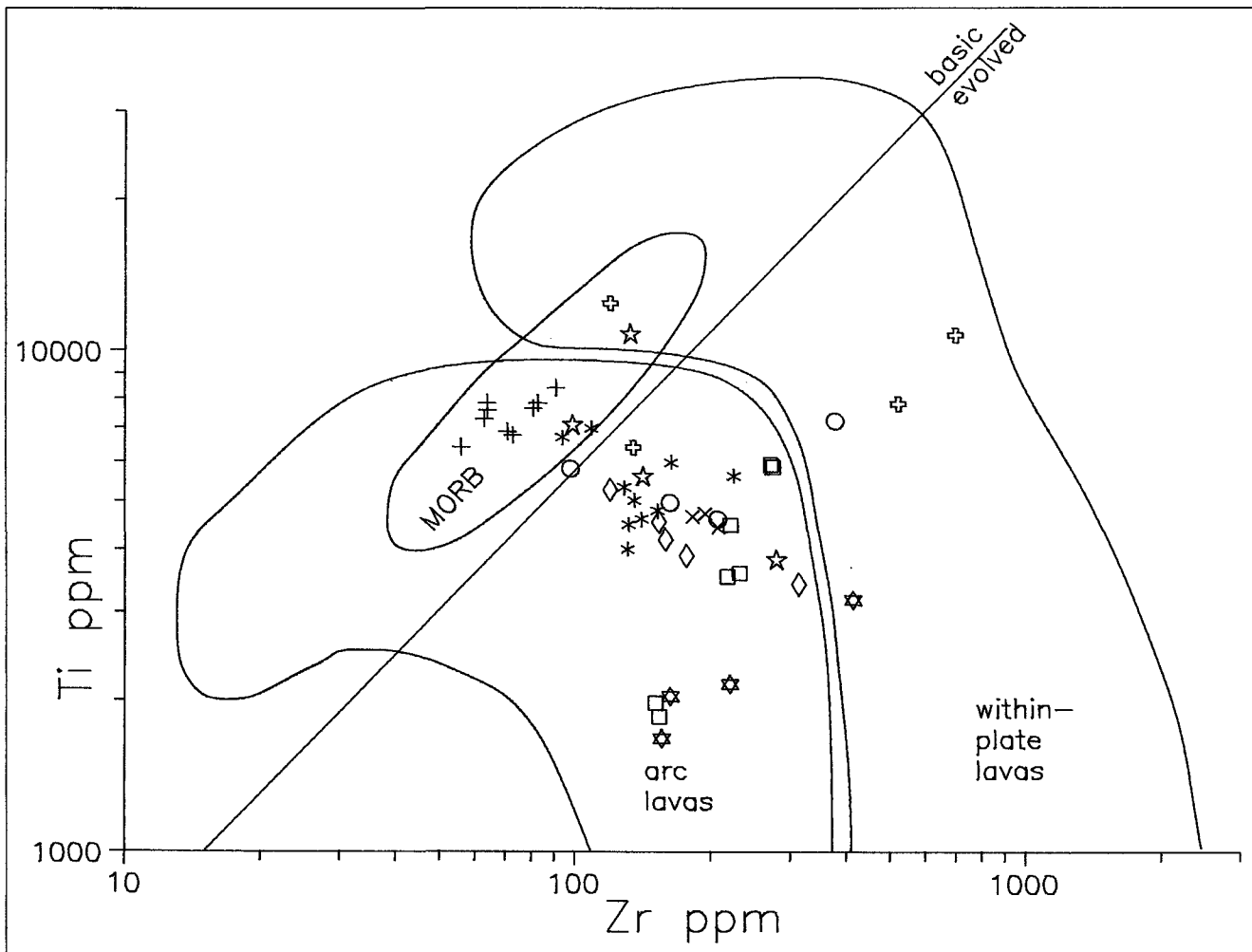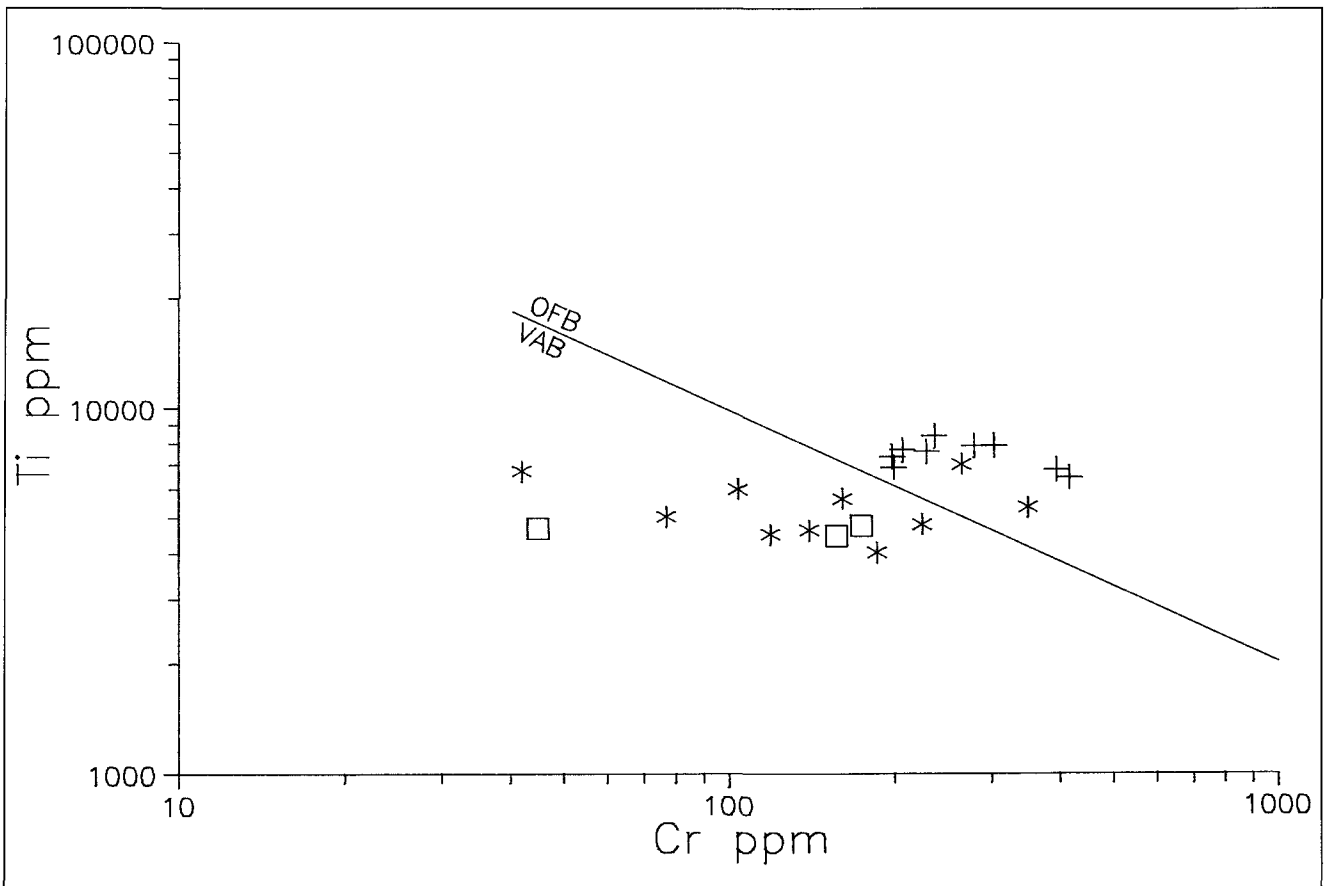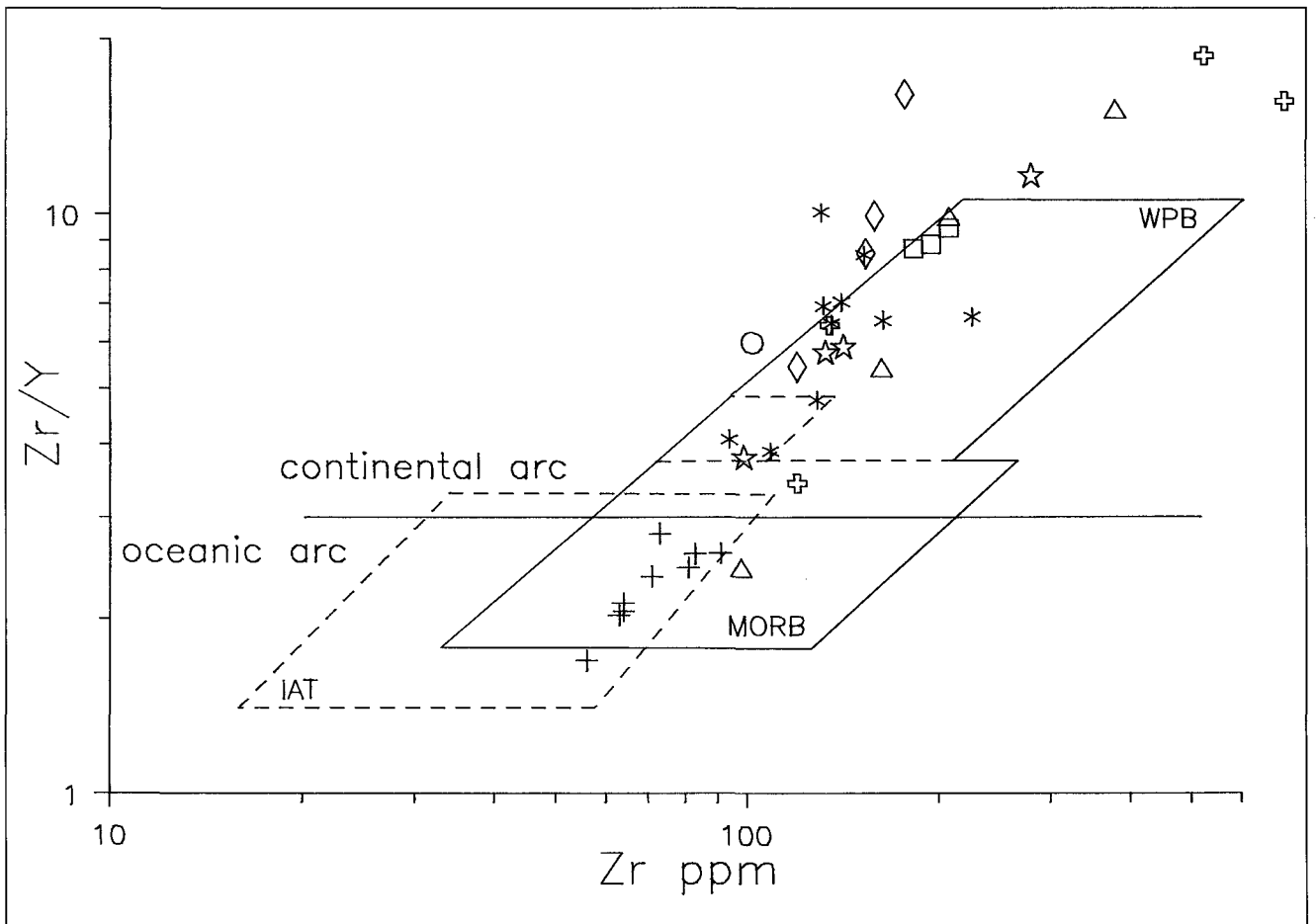
85

The former group is geochemically consistent with published data from the metagabbros or "Grobkornamphibolite" (HÖLL, 1975; JAHODA, 1984; TRUDU, 1984). The latter has a flat REE normalized pattern (Fig. 7a, U367) slightly enriched compared with the REE patterns of the fine-grained amphibolites. The same holds for the rock/MORB pattern (Fig. 8a, U367). They resemble the geochemistry of MORB and could be interpreted as Fe-Ti-basalts or high level gabbros(?) within the MORB-like fine-grained amphibolites.

Fine-grained amphibolites (49–53 % SiO_2, Tab. 1;4–6) are the most important rock type in the LMS (Fig. 2). They are tholeiitic in chemistry (with hypersthene or even quartz in the CIPW norm). Their high Y/Nb-ratio (>10) confirms their tholeiitic character (PEARCE & CANN, 1973). In the Ti-Zr-Y diagram (Fig. 3), most samples plot in field B, only three of the analyses are close to field A. This is consistent with an interpretation of these amphibolites as former MORBs or volcanic arc basalts. This plot, developed by PEARCE & CANN (1973) in order to discriminate between ocean-floor basalts, within-plate basalts and different types of island arc basalts, allows no clear distinction between calc-alkali basalts and ocean floor basalts. The same is true with the Ti vs Zr diagram (Fig. 4, PEARCE, 1980) and the Zr/Y vs Zr diagram (Fig. 5, PEARCE & NORRY, 1979). In both diagrams the analyses plot in the MORB field but overlap with the fields of volcanic arc lavas. A very useful diagram for distinguishing ocean-floor and oceanic island arc basalts is a plot of Ti vs Cr (PEARCE, 1975), in which the analyses clearly fall in the field of ocean-floor basalts (Fig. 6).

The geotectonic environment of the fine-grained amphibolites is highlighted by use of the REEs. The chondrite normalized pattern of the samples (U268 and U411) in (Fig. 7a).

For the same samples the rock/MORB diagram (PEARCE, 1982, 1983) shows a flat pattern with relative element abundances between Ta and Cr close to unity or just below (Fig. 8a). Only K, Rb, Ba and Th show a selective enrichment, while Sr is close to a MORB value. It should be noted that the enrichment of Rb is significantly more pronounced compared with K and Ba, thus forming a Rb peak. The Rb peak is typical of the immediate surrounding of the scheelite deposit. The samples farther away from the mineralization have the lowest relative enrichment in these elements similar to MORB like rocks described from other localities of the Habach Formation by STEYRER & HÖCK (1985) and PESTAL (1983). This Rb peak is not observed in the UMS. It is restricted to the vicinity of the mineralization but there it is observed in all rock types (e.g fine-grained amphibolite, hornblende-biotite-plagioclase schist, biotite gneiss). Therefore, most Rb values and possibly some K, Ba and also Th values can be ascribed to a later hydrothermal process. But some primary enrichment

of the LIL elements due to the origin of the basalts in a subduction-related environment cannot be excluded. Taking all data into account the interpretation of the fine-grained amphibolites as MORBs – possibly with a supra-subduction zone component – seems to be the most appropriate one.

This is corroborated by the Th-Hfx3-Ta diagram (WOOD et al., 1979), where the points plot in the VAB field but are less enriched in Th compared with the other rocks (Fig. 9).

One sample of amphibolites with hornblende phenocrysts (U291) differs markedly from the fine-grained amphibolites in having significantly higher abundances of P_2O_5, Nb, Zr the LIL-elements and the light REEs (Fig. 7b), but are lower in TiO_2 and Y (Tab. 1;7). Ti-Zr-Y (Fig. 3) and Ti vs Zr plots (Fig. 4) exhibit a more calc-alkaline character. The geochemical pattern (U291 in Fig. 8b) shows an enrichment of the LIL-elements (apart from the Rb-peak) which is distinctly above the range of the fine-grained amphibolites. Th, Ta, Nb, P_2O_5 and Ce are enriched, whereas TiO_2, Y and Yb are relatively depleted. The shape of the element distribution pattern is similar to that of the more intermediate rocks in the LMS (see chapter 3.1.2), but the MORB-normalized values are generally lower except for the compatible elements Sc and Cr. Similar features are observed in the rock/chondrite pattern (Fig. 7b) with an enrichment of the LREE with respect to HREE. The normalized values for the LREE are somewhat lower than those of the intermediate members of the LMS or the UMS volcanic rocks. Several element ratios such as Zr/Ti or Zr/Y combined with the shape of the rock/MORB or rock/chondrite patterns argue for a continental island arc environment. Such a pattern has been interpreted by PEARCE (1982, 1983) in terms of the rock/MORB diagram as island arc characteristics superimposed on a within-plate pattern.

3.1.2. Intermediate and acidic members

According to their SiO_2, abundances the intermediate to acidic rocks of the LMS range from 57 % to 79 %. The more basic to intermediate rocks are the plagioclase amphibolites (57 % SiO_2, Tab. 1;8,9), (garnet)-hornblende-biotite-plagioclase schists (54– 59 %, Tab. 1;10,11) and in part biotite gneisses ranging from 58–63 % SiO_2 (Tab. 1;12,13). The more acidic rocks comprise the remaining biotite gneisses (67–73 %, Tab. 1;14) and the albite gneisses (66– 79 % SiO_2, Tab. 1;15). Despite the wide range in the SiO_2, concentrations between the rocks a gap between 63 und 66 % SiO_2, is typical. This has also been observed by STEYRER (1982) and FRISCH & RAAB (1987). It must be emphasized here that most of these rocks show some evidence of their intrusive character: they form discordant dikes in the fine-grained MORB-like amphibo-

a)

Rock/Chond.

100

U367

U411

10

U268

1

La Ce Pr Nd Pm Sm Eu Gd Tb Dy Ho Er Tm Yb Lu

b)

Rock/Chond.

ooooo U291
ᴬᴬᴬᴬᴬ U304
••••• U334
▪▪▪▪▪ U424
***** U412

100

10

1

La Ce Pr Nd Pm Sm Eu Gd Tb Dy Ho Er Tm Yb Lu

c)

Rock/Chond.

U191

U173
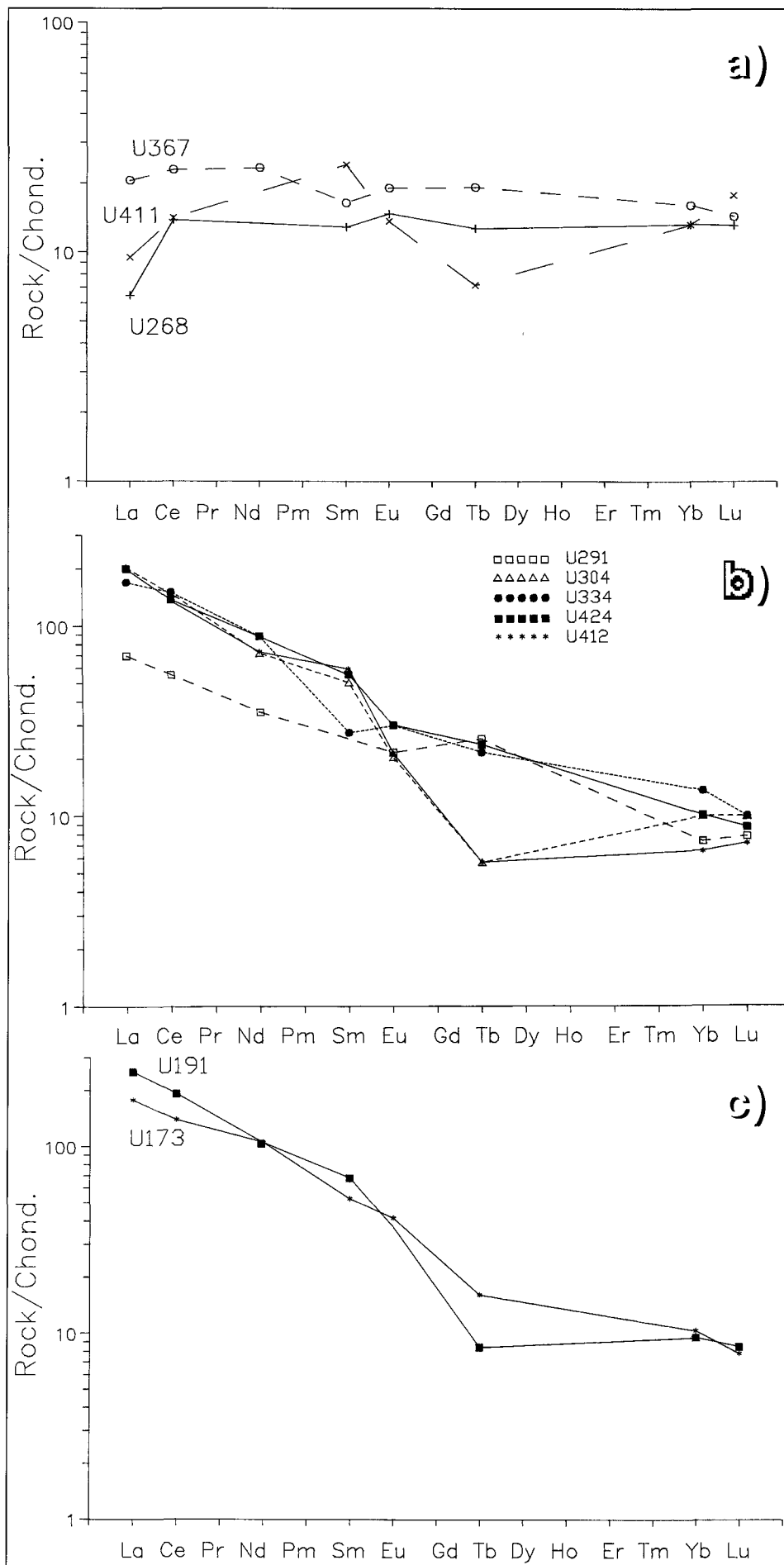
100

10

1

La Ce Pr Nd Pm Sm Eu Gd Tb Dy Ho Er Tm Yb Lu

Fig. 7.
Rock/chondrite patterns of the RE elements.
a) Flat, 10 -20 times enriched REE distribution for the fine-grained amphibolites (U268 and U411) and a relative Fe, Ti-rich medium-grained amphibolite (U367).
b) LREE enriched patterns for the basic/intermediate, intermediate and acidic members of the LMS (group II). U291, an amphibolite with hornblende phenocrysts shows the lowest LREE enrichment, all others have approximately 200 times enriched La and Ce normalized values. U424: plagioclase amphibolite, U412: (garnet)-hornblende-biotite-plagioclase schist, U304, U334: biotite gneiss.
c) LREE enriched patterns for the UMS. The patterns are almost identical with group II patterns of the LMS in Fig. 7b. U191 : biotite-epidote-albite schist, U173: prasinite.

lites, or they contain fragments of the older rocks (KRAIGER, 1989).

According to their geochemistry two groups can be distinguished among the intermediate and acidic rocks of the LMS. Group I (2–3 vol % of the LMS) with a tholeiitic character and low K contents includes some biotite gneisses and the albite gneisses (Tab. 1;15). Group II with a low Fe/Mg ratio and a calc-alkaline character includes the plagioclase amphibolites, the amphibolites with hornblende phenocrysts, the garnet-hornblende-plagioclase schists and the remaining biotite gneisses (Tab. 1;8–14). They comprise approximately 10 to 15 volume % of the total LMS.

The geochemical differences between both groups are more pronounced in their trace element geochemistry. The rocks of group I are characterized by low Nb, but somewhat higher Y concentrations and consequently lower Zr/Y ratios at a given Zr content, a lower $P_2O_5 \times 10^3/Y$ (<6), lower Ti and a higher Zr/Nb ratio (>25) compared with group II. A plot of Nb vs Y (Fig. 10a) is particularly usefull in demonstrating the separation between both groups.

Fig. 8.
Rock/MORB patterns.
a) For the fine-grained and medium-grained amphibolites the patterns show a distribution around unity between Ta and Cr. Note the strong enrichment of Rb close to the area of mineralization. K, Ba and Th are enriched. Samples as in 7a.
b) Zig-zag patterns for group II rocks of the LMS with enrichment of the elements from Sr to Sm and a depletion from Ti to Cr. This pattern is typical for island arc volcanics erupted on a continental crust (PEARCE, 1983). The amphibolite with hornblende phenocrysts shows less enrichment. Samples as in 7b.
c) Rock/MORB pattern for the UMS. The similar zig-zag pattern as in Fig. 8b and a similar enrichment trend is obvious. Samples as in Fig. 7c.

This diagram has been originally developed by PEARCE et al. (1984) in order to discriminate between different tectonic settings of granitic rocks. Since probably most of these intermediate to acidic rocks are dikes, the diagram must be interpreted with some caution according to its original designation. All samples (both groups) plot in the field of VAG (volcanic arc granites). Suprasubduction zone ocean ridge granites (SSZ-ORG) may also plot in the same field, close to the boundary between ORG and VAG.

For this reason the group I rocks are believed to have some affinities with SSZ-ORGs (plagiogranites), an interpretation which is supported by their relatively low K_2O, Rb and Ba but high Na_2O compared with group II. This results in rock/ORG patterns (Fig. 11) similar to ocean ridge granites in the sense of PEARCE et al. (1984), but distinct from those of VAGs. Their concentration of elements such as Nb, Zr, Y, K, and Ba are low, but higher as in typical plagiogranitic rocks (PEARCE et al., 1984). The values are comparable with some rhyolites from the Alley unit (rifting event) in Oman (ALABASTER et al., 1982), which also show some enrichment of these elements. Again the high Rb contents and possibly the Th and Ce anomalies in the rock/ORG pattern of sample
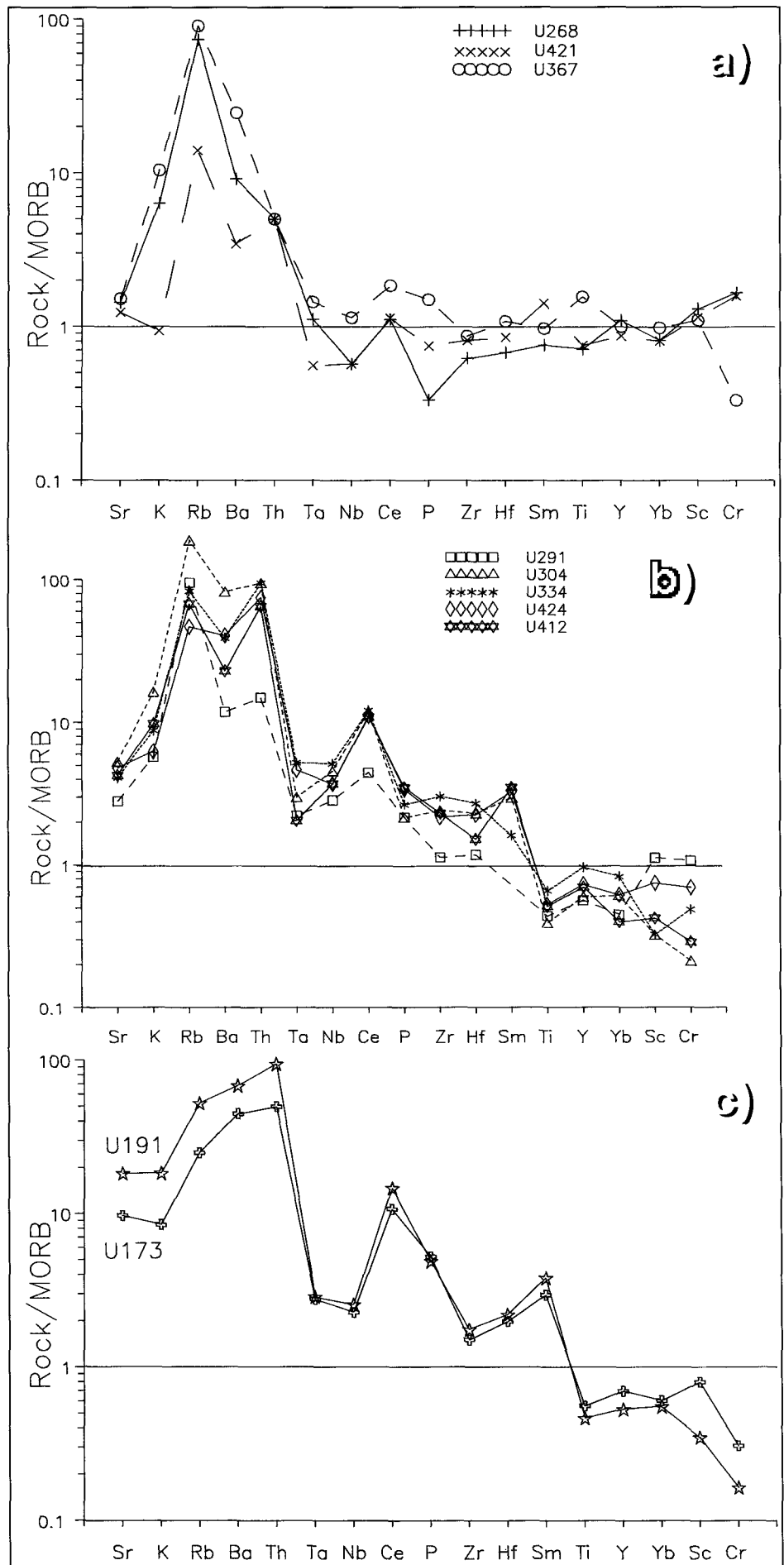
Fig. 9.
Th–Hf×3–Ta diagram according to Wood et al. (1979).
All analyses plot in the field of VAB (volcanic arc basalt). The fine-grained amphibolites
(thin crosses) show the slightest enrichment in Th. As other element concentrations
and ratios are indicative of a MORB character, the Th enrichment can be interpreted as
of secondary origin. All other analyses plot on the Th-rich side of the VAB field.
Symbols: LMS (group II): × = plagioclase amphibolite; ○ = amphibolite with horn-
blende phenocrysts; □ = biotite gneiss.
UMS: ● = prasinite; ■ = biotite-epidote-albite schist.
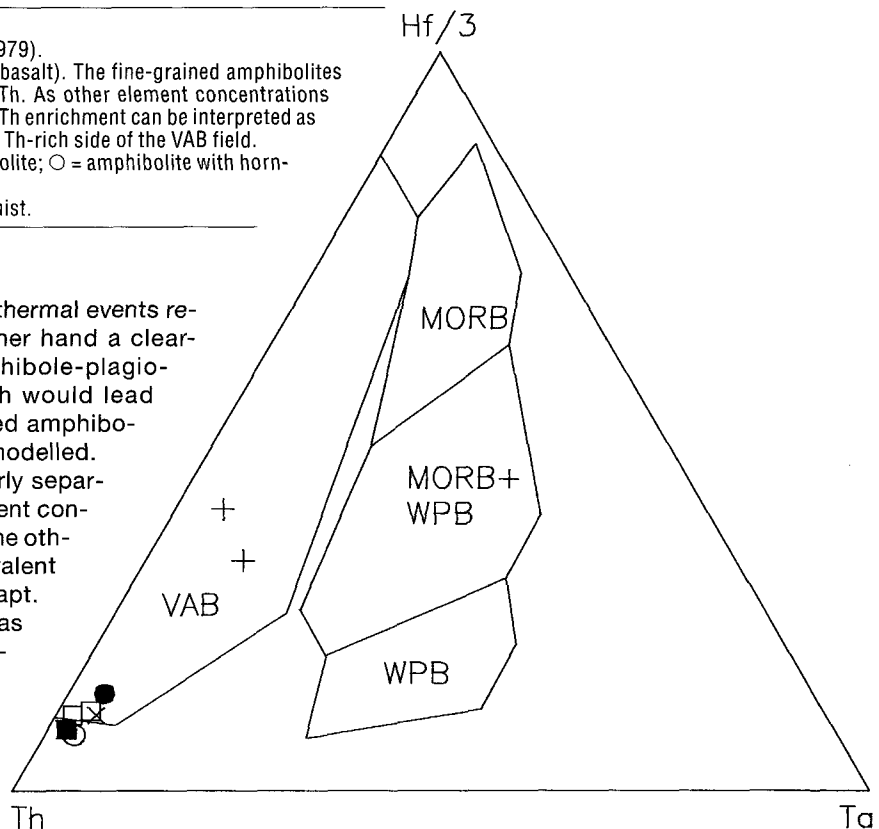
U235 could be due to some later hydrothermal events re-
lated to the mineralization. On the other hand a clear-
cut fractionation model (e.g. an amphibole-plagio-
clase-magnetite fractionation), which would lead
directly from the MORB-like fine-grained amphibo-
lites to the group I gneisses cannot be modelled.

As mentioned above, group II is clearly separ-
ated from group I rocks by several element con-
centrations and element ratios, but on the oth-
er hand there is no difference to equivalent
rocks from the UMS as shown below (chapt.
3.2). This is true for the major elements as
well as for most of the trace elements ex-
cept for Rb, which is selectively en-
riched in the mineralized area.

In the conventional trace element
plots such as Ti–Zr–Y (Fig. 3) the Ti
vs Zr (Fig. 4) or the Ti vs Cr
(Fig. 6), they plot in or close to
the fields of volcanic arc ba-
salts. In the Ti vs Zr diagram they form a trend with increas-
ing Zr and decreasing Ti similar to that described by SEE-
MANN & KOLLER (1989), probably due to the incoming of
magnetite as fractionated phase. This is also documented
in the Ti–Zr–Y diagram, where the analyses plot towards
the Zr apex. This relative enrichment in Zr has also a bear-
ing on the Zr/Y vs Zr diagram (Fig. 5), where the same ana-
lyses plot in or close to the within-plate field. In the Th–
Hf×3–Ta diagram (WOOD et al., 1979) the analyses plot on
the Th-rich side of the field for magmas from destructive
plate margins (VAG field in Fig. 9). In the AFM diagram
(Fig. 12) the group II magmas form, together with the lavas
from the UMS discussed below, a broad array following a
calc-alkaline trend.

All LIL elements in the MORB-normalized element pat-
terns of the basic-intermediate and intermediate rocks
(U291, 304, 334, 412, 424 in Fig. 8b) are significantly en-
riched, as are Ta, Nb, Zr, P, Hf, Sm while Ti, Y, Yb and the
compatible elements Cr and Sc are depleted. The enrich-
ment and depletion respectively is less pronounced in the
more basic rocks such as U291 compared with intermedi-
ate and acidic compositions. This is due to a higher de-
gree of fractional crystallization of clinopyroxene, amphi-
bole and plagioclase in SiO₂-rich volcanics (PEARCE &
NORRY, 1979).

The REE normalized patterns (Fig. 7b) are characterized
by a 150–200 times enrichment of the LREE and a relative
depletion of the HREE. Again, the most basic sample
U291 shows a small enrichment but the same general
shape. All these features including the high Zr/Y ratio (>6)
argue for calc-alkaline high K-basalts and andesites
which originated on a continental island arc (EWART, 1982;
PEARCE, 1982, 1983). For this reason the intermediate to
acidic rocks of group II in the LMS are best interpreted as
calc-alkaline to high-K continental island arc magmatic
rocks.

3.2. Upper Magmatic Sequence and "Habachphyllitentwicklung"

Among the rocks of the UMS and the overlying HPhE six
rock types, which are thought to be of magmatic origin,
have been investigated geochemically: biotite amphibo-
lite (45–53 % SiO₂, Tab. 2;1,2), prasinite (49–59 %,
Tab. 2;3), chlorite-albite schist (51–60 %, Tab. 2;4), bio-
tite-epidote-albite schist (59–53 %, Tab. 2;5,6), musco-
vite-epidote-albite schist (51–66 %, Tab. 2;7) and musco-
vite-albite gneiss (69–73 % SiO₂, Tab. 2;8).

The overall SiO₂-content ranges broadly from 45 to
74 %, although there is again a gap between 62 and 67 %.
The almost complete absence of volcanics in this SiO₂,
range (dacitic to rhyodacitic rocks) has already been re-
cognized (STEYRER, 1982; PESTAL, 1983) and seems to be
significant for the metavolcanic rocks of the Habach For-
mation (see also chapt. 3.1.2).

3.2.1. Basic and basic/intermediate members

As can be seen in the AFM-diagram (Fig. 12), the sam-
ples with a SiO₂, content < 56 % scatter broadly around a
calc-alkaline trend as the group II magmas from the LMS.
According to their relatively low Y/Nb ratios, varying with a
few exceptions from .6 to 6 , combined with a very low
Zr/P₂O₅ ×10⁴ ratio (.025 to .050) most of these rocks can
be classified as transitional between tholeiites and alkali-
basalts (PEARCE & CANN, 1973; FLOYD & WICHESTER, 1975;
PEARCE, 1982). The variable but generally lower Zr/Nb ratio
(7–20) compared with the metabasalts from the LMS is
consistent with this classification (ERLANK & KABLE, 1976;
PEARCE & NORRY, 1979).

On the Ti vs Zr diagram (Fig. 4) most samples show a
decrease of Ti with increasing Zr content, indicating a
fractionation process involving magnetite. In the most
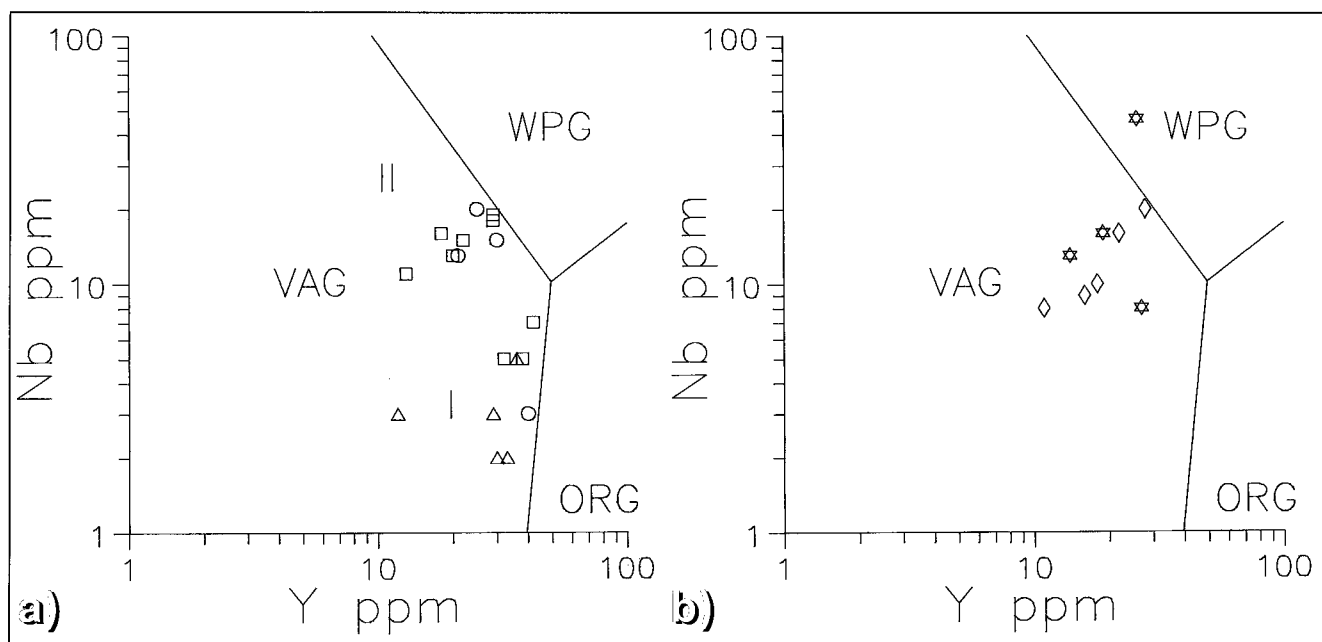acidic volcanic rocks e.g. the muscovite-albite gneisses,

Fig. 10.
Nb vs Y diagrams.
a) Nb vs Y diagram for the LMS.
   Two groups within the intermediate to acidic rocks in the LMS can be identified. I: group I, low in Nb (VAG field close to ORG); II: group II, high in Nb (VAG field close to WPG).
b) Nb vs Y diagram for the UMS.
   The intermediate to acidic rocks of the UMS plot in the same area as group II in the LMS.
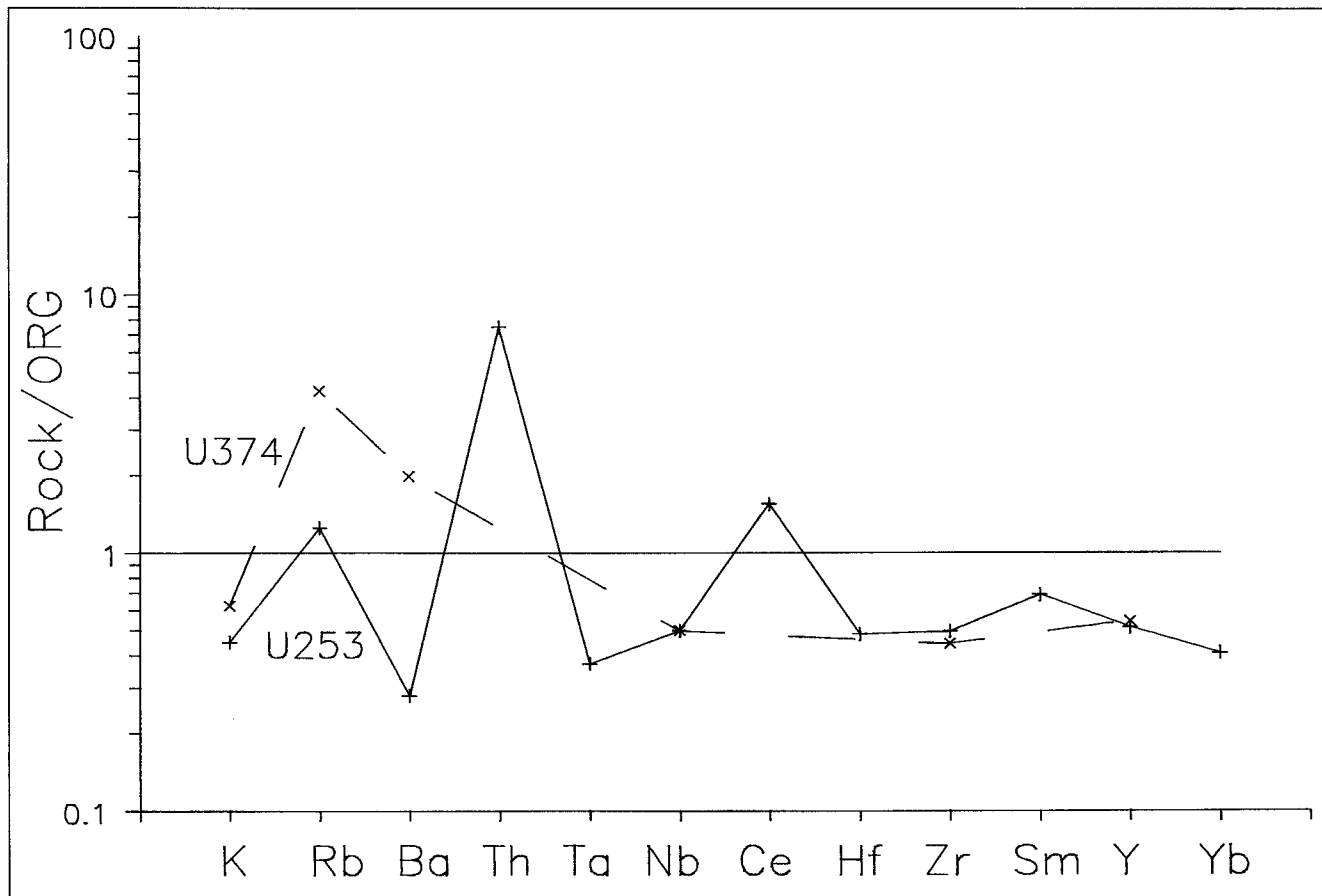Symbols as in Fig. 4, open triangles: albite gneiss VAG: volcanic arc granite; WPG: within-plate granite; ORG: ocean ridge granite.

Fig. 11.
Rock/ORG pattern of acidic members of group I rocks in the LMS.
The flat patterns argue for an oceanic origin of these rocks (plagiogranites ?).
U253: albite gneiss; U374: biotite gneiss.

Fig. 12.
AFM diagram of group II rocks of the LMS and the UMS. They form a broad calc-alkaline trend.
Symbols as in Fig. 4.
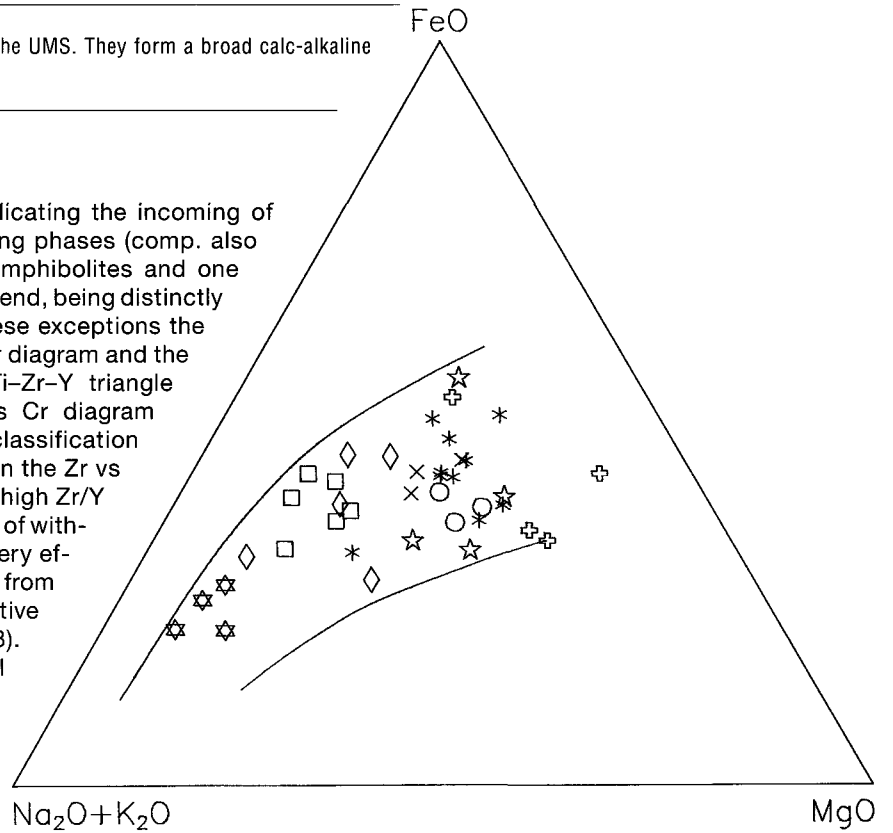
Zr and Ti decrease simultaneously indicating the incoming of biotite and/or amphibole as fractionating phases (comp. also SEEMANN & KOLLER, 1989). Only few amphibolites and one chlorite-albite schist do not follow this trend, being distinctly enriched in Ti and/or Zr. Apart from these exceptions the fractionation trend observed in the Ti/Zr diagram and the distribution of the analyses in the Ti–Zr–Y triangle (PEARCE & CANN 1973) and the Ti vs Cr diagram (PEARCE, 1975) are consistent with the classification as calc-alkaline basalts (Fig. 3 and 6). In the Zr vs Zr/Y-diagram (Fig. 5) according to their high Zr/Y ratio most of the samples plot in the field of within-in-plate basalts. This plot produces a very effective discriminant between basalts from oceanic arcs and basalts erupted at active continental margins (PEARCE, 1983). Oceanic-arc basalts plot in the original island arc tholeiite field, whereas continental-arc basalts plot towards higher Zr/Y ratios, i.e. in the original within-plate field indicated by the horizontal line at a Zr/Y ratio of 3.

The strong increase of the Zr/Y ratios from 4 to >12 is not only restricted to the UMS but has been noted already by STEYRER & HÖCK (1985) and can be observed also in some data sets published by FRISCH & RAAB (1987).
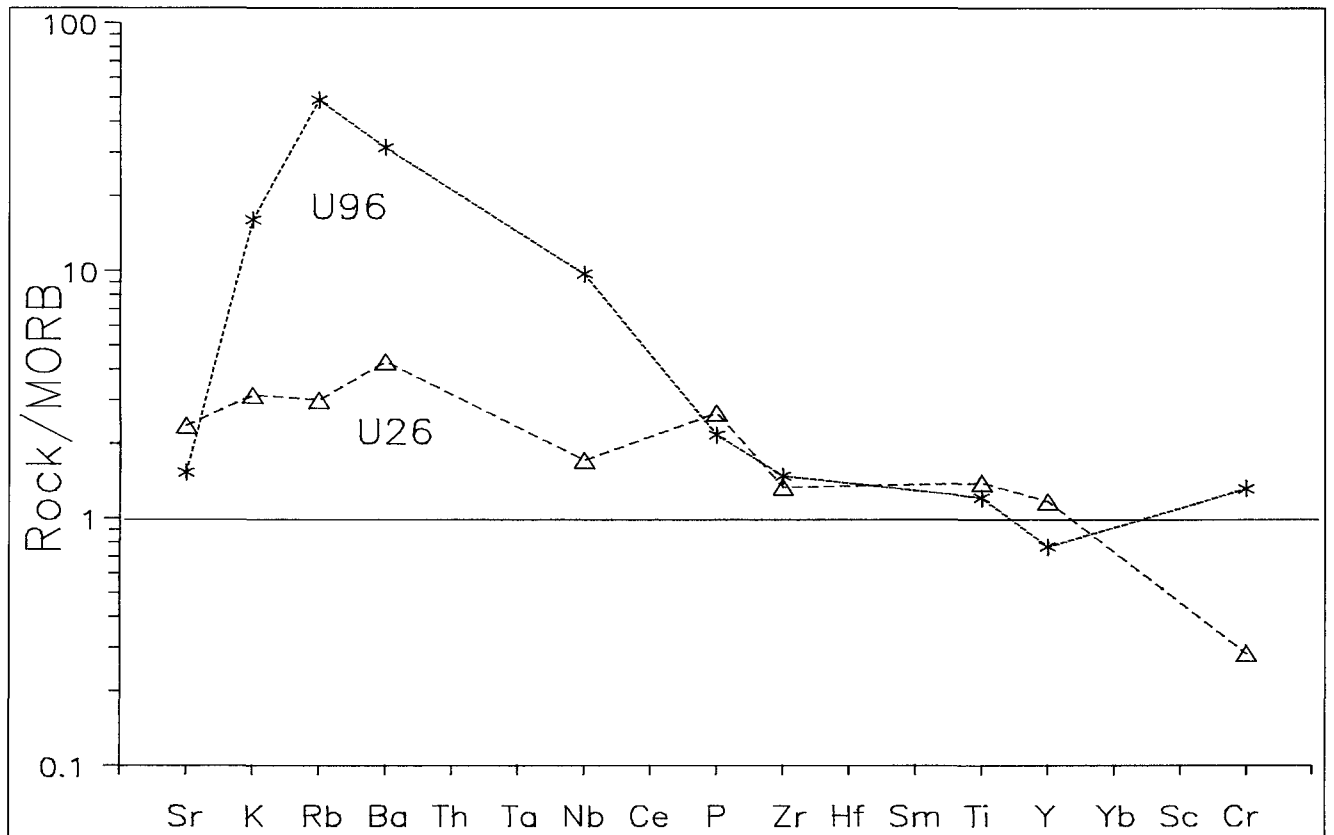

Fig. 13.
Rock/MORB diagram for two rocks from the UMS.
They show hump patterns unlike those in Fig. 8. This distribution is more typical of a within-plate environment (PEARCE, 1982). The different enrichment could reflect a tholeiitic and alkaline within-plate character respectively.
U26: biotite amphibolite; U96: chlorite-albite schist.

Normalized against an average MORB (U173, U191 in Fig. 8c), the elements exhibit a characteristic zig-zag pattern distinctly enriched from Sr to Sm (PEARCE, 1983). The enrichment of the LIL-elements and of P are believed to be typical of calc-alkaline to shoshonitic island arc volcanic rocks (PEARCE, 1982). However, the 2 to 5-fold enrichment of Nb and Ta as the 1.5 fold enrichment of Zr can not be explained as "subduction component". Nb, Ta, Zr and Hf are assumed by PEARCE (1983) to be derived for the most part from a trace element enriched metasomatized subcontinental lithosphere and can be characterized therefore as "within-plate component". This pattern combined with the strong enrichment of Nb and Ta relative to Zr and Y resulting in the relatively low Y/Nb and Zr/Nb ratios respectively indicates an origin of the basalts and basaltic andesites in a continental island arc environment.

Rock/MORB patterns of some of the biotite-rich amphibolites from the UMS, e.g. U155 in Tab. 2;2 are similar to those of continental island arcs described above, but are shifted towards higher absolute abundances. This indicates a greater contribution of the enriched subcontinental lithosphere to the melt. Due to the high K_2O-values of the metabasites and their enriched patterns, they may be classified as absarokites (basaltic rocks of shoshonite series, PECCERILLO & TAYLOR 1976).

On the other hand, two samples (one amphibolite U26 and one chlorite-albite schist U96 from the HPhE in Tab. 2;1,4) show characteristics of within-plate basalts (Fig. 13) with the typical "hump" pattern observed in many tholeiitic and alkalic basalts (PEARCE, 1980, 1983). According to their different degree of enrichment highlighted by the varying Y/Nb-ratio, they can be interpreted as alkaline (U96) or as tholeiitic (U26) within-plate basalts.

3.2.2. Intermediate and Acidic Members

As mentioned above, the intermediate to acidic rocks from the UMS and the HPhE split up into an andesitic (56–60 % SiO_2) and a rhyolitic (68–74 % SiO_2) group. The andesites exhibit relatively high concentrations of Sr,Rb, Ba, P, Ni and Cr as well as high ratios for Zr/Y, Rb/Sr and Ba/Sr, whereas Y, K/Rb and K/Ba are relatively low. According to the compilation by BAILEY (1981), such a geochemical pattern would be consistent with andesites formed at a continental island arc. The geochemical composition of the rhyolitic group shows similar characteristics and can be better compared with rhyolites derived from a continental island arc (e.g. North Central America, CARR et al., 1982), than with those formed in an oceanic island arc regime (e.g. Oman, ALABASTER et al., 1982). Finally it should be noted, that the andesites and rhyolites plot in the same area as group II of the intermediate to acidic rocks in the LMS on a Nb vs Y diagram (Fig. 10b), thus supporting a close geochemical relationship between both groups.

4. Discussion

Comparing the petrographic (KRAIGER, 1987, 1989) and the geochemical results presented in this paper, it becomes clear that the two magmatic sequences originated from two different tectonic settings. The protoliths of the fine-grained amphibolites (LMS) resemble ocean floor basalts and probably formed in a subduction influenced marginal oceanic basin. This is indicated by the concentrations of Ti, Zr, Hf, Nb, Ta, P_2O_5, Y, Cr and the flat REE pattern.

The enrichment of the LIL elements apart from the Rb-anomaly points towards a subduction influence. The occurrence of intercalated gabbroic rocks (medium-grained amphibolite) and of cumulate clinopyroxenites (hornblendites), combined with the overall geochemical uniformity of the fine-grained amphibolites indicates a subvolcanic origin of these rocks (see also KRAIGER, 1989). This interpretation is supported by the occurrence of similar rocks in the Habach valley, W of the scheelite mine where remnants of chilled margins are still visible. Among the dike rocks, the mostly acidic rocks of group I might be interpreted with caution as plagiogranite. For this reason the LMS is believed to be a remnant of a sheeted dike complex. However, the majority of the intermediate to acidic rocks of the LMS (group II) can not be derived from an ocean ridge magma. They are calc-alkaline in their geochemical composition and represent rather a separate magmatic evolution corresponding to a later continental island arc magmatism. These calc-alkaline rocks are thought to be intrusive in character, forming dikes rather than volcanic layers. Apart from the general considerations regarding the intrusive character of the LMS rocks and their calc-alkaline intercalations, this idea is supported by a few discordant dikes and inclusions of basic country rocks in the intermediate to acidic members.

The UMS, resting unconformably on the LMS, is composed of basic to acidic metavolcanics and contains only minor metasediments. Restricted to the uppermost section (HPhE) different types of metasediments, such as phyllites and quartzites, predominate over rare metavolcanic rocks. Geochemically, the metavolcanics of the UMS resemble calc-alkaline to shoshonitic volcanic rocks ranging from basaltic to rhyolitic in compositions. Their chemical signature over the whole range of SiO_2, values points uniformly to a continental island arc environment. This contrasts markedly with the tectonic setting of the former LMS basalts, but is consistent with the intermediate to acidic dikes in the LMS. Comparing the geochemistry, different element ratios and spider diagrams (rock/chondrite; rock/MORB) of the UMS with group II magmatic rocks in the LMS as exemplified in Fig. 7 b,c, and Fig. 8 b,c. it becomes obvious how close both volcanic series are related to each other. Even in the absence of reliable age determination this suggests a close genetic connection. The magmatic activity in the UMS has probably ended with the eruption of basalts of within-plate character, forming thin layers of amphibolites in the HPhE.

It should be noted finally, that FRISCH & RAAB (1987) report geochemical analyses of metabasites and metaandesites of the Habach Formation (Tauernkogel, Weinbühel) that compare well with the calc-alkaline rocks of the LMS. These authors believe the concentrations of Ti, P and Zr to be of secondary origin, due to passive enrichment during deformation and recrystallization. However, detailed petrographic investigations by KRAIGER (1987, 1989) have shown that:

1) There are no differences in deformation such as shear zones between the tholeiitic and the calk-alkaline rocks of the LMS, and

2) higher abundances of P and Ti are probably related to higher primary contents of Ti-rich clinopyroxenes or Ti-amphiboles, which can be observed as pseudomorphs containing epidote, sphene and apatite inclusions.

Moreover, a passive 2–5 times enrichment of sphene, apatite and zircon by the mechanism proposed by FRISCH

& RAAB (1987) should have led to extreme modifications in the major element contents, which is not observed. On the contrary, it could be argued that the chemically modified rocks of FRISCH & RAAB (1987) also represent rocks of a continental island arc.

5. Conclusions

According to the petrographic and geochemical features described above, the following two-stage genetic model is proposed.

In the vicinity of an older continental margin, a marginal basin has been formed, of which the hornblendites, the medium- and fine-grained amphibolites and group I rocks of the LMS (possible dismembered ophiolites) are thought to represent the floor. According to U/Pb dating of some amphibolites from the LMS by v. QUADT (1985, 1992), the formation of this basin could have taken place in the range of 535–500 Ma. During the subsequent closure of this ocean basin, the crust was tectonically sliced and in part emplaced onto the continental crust. Furthermore, volcanic rocks of a continental island arc origin were deposited on, and in part intruded the older oceanic crust (LMS). The former build up the UMS today, the latter represent the calc-alkaline intrusive parts of the LMS. The decrease of volcanic rocks and the increase of sedimentary rocks in the uppermost part of the sequence (HPhE) mark the end of the subduction process responsible for generating the calc-alkaline magmatism interpretated as arc magmatism. Finally, small amounts of within-plate basalt were erupted, whose composition was influenced by the subcontinental lithosphere.

This model is based on the close geochemical similarity of the volcanics of the UMS with group II (probably intrusive) intermediate to acidic rocks of the LMS and assumes a close genetic relationship between both magmatic sequences. The model therefore implies that the continental island arc sequence as a whole is younger than the ophiolites. This is obviously not in agreement with the paleontological findings by REITZ & HÖLL (1988), who described acritarchs of probably Vendian age from the Habach phyllites (HPhE). Field evidence suggests a close relationship between the Habach phyllites and the UMS especially in the Habach valley (STEYRER, 1983; PESTAL, 1983). As a consequence the UMS should be of Upper Proterozoic age also. BRIEGLEB (1991) postulated an evolution model in some respects similar to the one presented here but arguing that the two calc-alkaline sequences in the LMS (group II) and the UMS respectively are of different age (the first being significantly younger and thus not related genetically to the second).

VAVRA (1989) and VAVRA & HANSEN (1991) presented some evidence based on U-Pb dating that the UMS, at least in the area of the Habach valley and the Felber valley, is much younger than Upper Proterozoic and formed in the time range of the Variscan magmatism. This is based on a 334 Ma U-Pb age of a high-K metarhyolite from the Habach valley. The Variscan age is corroborated by two own, yet unpublished analyses from leucocratic gneisses (metarhyolites) with an U-Pb age of 350–360 Ma. The samples were taken from the Felber valley and the Hollersbach valley. Clearly more age data on the Habach Formation as a whole are needed for a consistent geodynamic interpretation. At the present stage the presented model seems to fit the data best.

References

ALABASTER, T., PEARCE, J.A. & MALPAS, J. (1982): The volcanic stratigraphy and petrogenesis of the Oman ophiolite complex. – Contrib. Mineral. Petrol., 81, 168–183.

BAILEY, J.C. (1981): Geochemical criteria for a refined tectonic discrimination of orogenic andesites. – Chem. Geol., 32, 139–154.

BECCALUVA, L., OHNENSTETTER, D., OHNENSTETTER, M. & PAUPY, A., 1984: Two magmatic series with island arc affinities within the Vourinos ophiolite. – Contrib. Mineral. Petrol., 85, 253–271.

BENCE, A.E & ALBEE, A.L. (1968): Empirical correction factors for the electron microanalysis of silicates and oxides. – J. Geol., 76, 382–403.

BICKLE, M.J. & PEARCE, J.A. (1975): Oceanic mafic rocks in the Eastern Alps. – Contrib. Mineral. Petrol., 49, 177–189.

BRIEGLEB, D. (1991): Ein epigenetisches Modell der Scheelitlagerstätte Felbertal (Land Salzburg. – Ber. Deutsch. Miner. Ges., Bh. EJM, 3, Nr. 1, S. 43.

CARR, M.J., WILLIAM, I.R & STOIBER, R. (1982): Central America. – In: R.S. THORPE, (ed.): Andesites, 149–166, John Wiley and Sons.

ERLANK, A.H & KABLE, E.J.D. (1976): The significance of incompatible elements in Mid-Atlantic Ridge basalts from 45°N with particular references to Zr/Nb. – Contrib. Mineral. Petrol., 54, 281–294.

EWART, A. (1982): The mineralogy and petrology of Tertiary recent orogenic volcanic rocks: with special reference to the andesitic- basaltic compositional range. – In: Andesites, R.S THORPE (ed.), 25–95, John Wiley and Sons.

FLOYD, P.A & WICHESTER, J.A. (1975): Magma type and tectonic setting discrimination using immobile elements. – Earth. Plan. Sci. Lett., 27, 211–218.

FRASL, G. (1958): Zur Seriengliederung der Schieferhülle in den Mittleren Hohen Tauern. – Jb. Geol. B.-A., 101, 323–472.

FRASL, G. (1960): Zum Stoffhaushalt im epi- bis mesozonalen Pennin der Mittleren Hohen Tauern während der alpidischen Metamorphose. – Geol. Rundsch., 50, 192–203.

FRISCH, W. & RAAB, D. (1987): Early Paleozoic back-arc and island arc settings in greenstone sequences of the central Tauern Window (Eastern Alps). – Jb. Geol. B.-A., 129, 545–566.

GILG, H.A., HÖLL, R., KUPFERSCHMIED, M.P., REITZ, E., STÄRK, H. & WEBER-DIEFENBACH, K. (1989): Die Basisschieferfolge in der Habachformation im Felber- und Amertal (Tauernfenster, Salzburg). – Mitt. österr. geol. Ges., 81 (1988), 65–91.

HAWKINS, J.W. Jr. (1980): Petrology of back-arc basins and island arcs: their possible role in the origin of ophiolites. – In: A. PANAIYOTOU (ed.): Proceedings International Ophiolite Symposium, Cyprus 1979, Geol. Surv. Cyprus, 244–254.

HÖCK, V. (1993): The Habach formation and the Zentralgneis – a key in understanding the Palaeozoic evolution of the Tauern window (Eastern Alps). – In: J.v. RAUMER & F. NEUBAUER (eds): The pre-Mesozoic Geology in the Alps, 359–372, Springer.

Höck, V. & Miller, Ch. (1987): Mesozoic ophiolite sequences and non-ophiolitic metabasites in the Hohe Tauern. – In: H.W. Flügel & P. Faupl (eds): Geodynamics of the Eastern Alps, 16–33, Deuticke Vienna.

Höck, V. & Pestal, G. (1990): Exkursion E4: Habachformation, Altkristallin im Habachtal und Felbertal. – Mitt. Österr. Min. Ges., **135**, 129–137.

Höll, R. (1975): Die Scheelitlagerstätte Felbertal und der Vergleich mit anderen Scheelitvorkommen in den Ostalpen. – Abh. Bayer. Akad. Wiss., math.-naturwiss. Kl., **157** A-B, München.

Jahoda, R. (1984): Das Westfeld der Scheelitlagerstätte Mittersill (Land Salzburg/Österreich) – Geologie, Petrographie und Vererzung in einem Profil durch die Lagerstätte. – Unveröff. Dipl-Arb. Univ. Leoben, 280 pp.

Kraiger, H. (1987): Geologie, Petrographie und Geochemie der Habachformation am Beispiel des Unterfahrungsstollens der Scheelitlagerstätte Felbertal, Salzburg. – Diss. Univ. Salzburg, 280 p.

Kraiger, H. (1989): Die Habachformation – ein Produkt ozeanischer und kontinentaler Kruste. – Mitt. Öst. Geol. Ges., **81**, 47–64.

Nisbet, E.G., Dietrich, V.H. & Esenwein, A. (1979): Routine trace element determination in silica minerals and rocks by X-ray fluorescence. – Fortschr. Min., **57**, 264–279.

Pearce, J.A. (1975): Basalt geochemistry used to investigate past tectonic environments on Cyprus. – Tectonophysics, **25**, 41–67.

Pearce, J.A. (1980): Geochemical evidence for the genesis and eruptive setting of lavas from Tethyan ophiolites. – In: Panayiotou, A. (ed): Ophiolites, Proc. Intern. Ophiolite Symp. Cyprus 1979, Geol. Surv. Cyprus, 261–272.

Pearce, J.A. (1982): Trace element characteristics of lavas from destructive plate boundaries. – In: R.S. Thorpe (ed.): Orogenic Andesites, John Wiley and Sons, New York, 525–548.

Pearce, J.A. (1983): Role of the sub-continental lithosphere in magma genesis at active continental magmas. – In: C.J. Hawkesworth & M.J. Norry (eds.): Continental basalts and mantle xenoliths, Shiva Geology Series, 230–272.

Pearce, J.A. & Cann, J.R. (1973): Tectonic setting of basic volcanic rocks determined using trace element analyses. – Earth Planet. Sci. Lett., **19**, 290–300.

Pearce, J.A., Harris, N.B.W & Tindle, A.G. (1984): Trace element discrimination diagrams for the tectonic interpretation of granitic rocks. – J. Petrol., **25**/4, 953–983.

Pearce, J.A. & Norry, M.J. (1979): Petrogenetic implications of Ti, Zr and Nb variations in volcanic rocks. – Contrib. Mineral. Petrol., **69**, 33–47.

Peccerillo, A. & Taylor, S.R. (1976): Geochemistry of Eocene calc-alkaline volcanic rocks from the Kastamonn area, Northern Turkey – Contrib. Mineral. Petrol., **58**, 63–81.

Pestal, G. (1983): Beitrag zur Kenntnis der Geologie in den Mittleren Hohen Tauern im Bereich des Amer- und Felbertales (Pinzgau, Salzburg). – Unveröff. Diss. Univ. Wien, 117 S.

Quadt, A. von (1985): Geochronologische, geochemische und isotopenchemische Untersuchungen an Beispielen der Habachformation, der Scheelitlagerstätte und des umgebenden Altkristallins im Felbertal (Land Salzburg). – Unveröff. Diss. ETH Zürich, 241 p.

Quadt, A. von (1992): U/-Pb zircon and Sm-Nd geochronology of mafic and ultramafic rocks from the central part of the Tauern Window (eastern Alps). – Contrib. Mineral. Petrol., **110**, 57–67.

Reitz, E & Höll, R. (1988): Jungproterozoische Mikrofossilien aus der Habachformation in den mittleren Hohen Tauern und dem nordostbayerischen Grundgebirge. – Jb. Geol. B.-A., **131**, 329–340.

Seemann, R. & Koller, F. (1989): Petrographic and geochemical investigations in the Knappenwand Area, Habach Formation (Tauern Window, Austria). – Mitt. österr. geol. Ges., **81**, 109–122.

Steyrer, H.P. (1982): Geochemie, Petrographie und Geologie der Habachformation im Originalgebiet zwischen äußerem Habachtal und Untersulzbachtal (Pinzgau, Salzburg). – Unveröff. Diss. Univ. Salzburg, 178 S.

Steyrer, H.P. (1983): Die Habachformation der Typlokalität zwischen äußerem Habachtal und Untersulzbachtal (Pinzgau/ Salzburg). – Mitt. österr. geol. Ges., **76**, 69–100.

Steyrer, H.P & Höck, V. (1985): Geochemistry of the metabasites in the Habachformation (Salzburg, Hohe Tauern, Austria). A preliminary report. – Ofioliti, **10**, H.2/3, 441–456.

Trudu, A.G. (1984): Petrology, structure and origin of the K1–scheelite orebody, westfield sector, Felbertal, Austria. – Unpubl. Thesis: Queens Univ. Kingston, Ontario, Canada.

Vavra, G. (1989): Die Entwicklung des penninischen Grundgebirges im östlichen und zentralen Tauernfenster der Ostalpen – Geochemie, Zirkonmorphologie, U/Pb-Radiometrie. – Tübinger Geowiss. Arb., Reihe A, Geol., Paläont., Strat., **6**, 150 p.

Vavra, G & Hansen, B.T. (1991): Cathodoluminescence studies and U/Pb dating of zircons in pre-Paleozoic gneisses of the Tauern Window: Implications for the Penninic basement evolution. – Geol. Rundsch., **80**/3, 703–715.

Wood, D.A., Joron, J.-L. & Treuil, M. (1979): A re-appraisal of the use of the trace elements to classify and discriminate between magma series erupted in different tectonic settings. – Earth Plan. Sci. Lett., **45**, 326–336.